Available online at www.sciencedirect.com

ScienceDirect

Physics Procedia 81 (2016) 77 – 80

Physics Procedia

28th International Symposium on Superconductivity, ISS 2015, November 16-18, 2015, Tokyo, Japan

Transverse Components of Flux Line Lattice Form Factors in Uniaxial Superconductors

Masanori Ichioka[a,]*, Yuujirou Amano[a], Masahiro Ishihara[a], and Kazushige Machida[b]

[a]*Department of Physics, Okayama University, Okayama 700-8530, Japan*
[b]*Department of Physics, Ritsumeikan University, Kusatsu 525-8577, Japan*

Abstract

Magnetic field orientation dependence of transverse and longitudinal flux line lattice form factors are theoretically studied in uniaxial superconductors with extremely large anisotropy ratio 60 for some field magnitudes. The form factors are estimated by two methods, the Eilenberger theory and the London theory comparatively. We also compare them to the form factors observed by the small angle neutron scattering experiment on Sr_2RuO_4. We discuss the cutoff function of extended London theory, and the contributions from the suppression of the pair potential as a function of the field orientation.

Peer-review under responsibility of the ISS 2015 Program Committee

Keywords: Flux line lattice form factor; Transverse field; Eilenberger theory; Extended London theory

1. Introduction

In uniaxial superconductors where the coherence length is anisotropic between the *c*-axis direction and the basal *ab*-plane, transverse fields appear among the internal magnetic field in the flux line lattice (FLL) states in type-II superconductors, when the magnetic field orientation is tilted from the *c*-axis or the *ab*-plane. The transverse FLL form factors are observed by the small angle neutron scattering (SANS) experiments on Sr_2RuO_4 [1]. The form factors are roughly estimated by the London theory [2]. For quantitatively reliable estimate, we have to perform

* Corresponding author. Tel.: +81-86-251-7806; fax: +81-86-251-7830.
E-mail address: ichioka@cc.okayama-u.ac.jp

Peer-review under responsibility of the ISS 2015 Program Committee
doi:10.1016/j.phpro.2016.04.031

heavy calculations by the Eilenberger theory in the vortex lattice states. In our previous study [3] in the case of anisotropy ratio $\gamma \sim 6$ corresponding to $YBa_2Cu_3O_{7\text{-d}}$ (YBCO), we showed that the cutoff function in extended London theory can be estimated from the results by the Eilenberger theory in the field orientation dependence of the FLL form factors. There, we also discussed dependence on the anisotropy ratio, and differences between the *s*-wave and the *d*-wave pairings. The effects of the pairing symmetry on the form factors come from the temperature dependence of the superfluid density. In this paper, we study the case of extremely large anisotropy ratio γ=60 corresponding to Sr_2RuO_4 in order to understand behaviors of the transverse fields. The FLL form factors by the Eilenberger theory [4] and the SANS experiment [1] are compared to those of the extended London theory.

2. Flux line lattice form factors in the London theory

In the crystal coordinate (*a*,*b*,*c*), magnetic field is tilted by θ from the *c*-axis. For the vortex structure, we use coordinate (*x*,*y*,*z*), where the *z*-axis is along the flux line direction. We consider a quasi-two-dimensional Fermi surface with rippled cylinder shape. The Fermi velocity is given by $\mathbf{v}=(v_a,v_b,v_c)\propto(\cos\phi,\sin\phi,\gamma^{-1}\sin p_c)$ on the Fermi surface at $\mathbf{p}=(p_F\cos\phi,p_F\sin\phi,p_c)$. The parameter γ=60 gives anisotropy ratio of the coherence length. We set unit vectors of the FLL as $\mathbf{u}_1=c_v(\alpha/2,\sqrt{3}/2,0)$ and $\mathbf{u}_2=c_v(\alpha/2,-\sqrt{3}/2,0)$ with $c_v^2=2\phi_0/(\sqrt{3}\alpha\bar{B})$, $\alpha=3\Gamma_\theta$, averaged flux density $\bar{B}$, the flux quantum ϕ_0, and $\Gamma_\theta=(\cos^2\theta+\gamma^{-2}\sin^2\theta)^{-1/2}$ of the effective mass model. Thus, wave vectors in the reciprocal space are given by $\mathbf{q}_{(h,k)}=h\mathbf{q}_1+k\mathbf{q}_2$ with integers *h* and *k*. Here $\mathbf{q}_1=2\pi c_v^{-1}(\alpha^{-1},-1/\sqrt{3},0)$ and $\mathbf{q}_2=2\pi c_v^{-1}(\alpha^{-1},1/\sqrt{3},0)$. The FLL form factors $\mathbf{B}(\mathbf{q}_{(h,k)})=(B_{x(h,k)},B_{y(h,k)},B_{z(h,k)})$ are obtained by Fourier transformation of the internal field distribution $\mathbf{B}(\mathbf{r})$ in the FLL state. We use Eilenberger unit [3,4] for length, magnetic field and energy in this paper.

In the London theory, FLL form factors for $\mathbf{q}_{(h,k)}$ are given by

$$B_{x(h,k)}=-\kappa^2 m_{yz}q_xq_yd^{-1}\bar{B},\quad B_{y(h,k)}=\kappa^2 m_{yz}q_x^2d^{-1}\bar{B},\ B_{z(h,k)}=(1+\kappa^2m_{zz}q^2)d^{-1}\bar{B} \tag{1}$$

with $d=\{1+\kappa^2(m_{xx}q_y^2+m_{yy}q_x^2)\}(1+\kappa^2m_{zz}q^2)-\kappa^4m_{yz}^2q^2q_x^2$ and $q^2=q_x^2+q_y^2$. Effective masses are given by $m_{xx}=m_a$, $m_{yy}=m_b\cos^2\theta+m_c\sin^2\theta$, $m_{zz}=m_b\sin^2\theta+m_c\cos^2\theta$, and $m_{yz}=(m_b-m_c)\sin\theta\cos\theta$, where $m_i^{-1}=2T\sum_{\omega_n>0}\langle\hat{v}_i^2\Delta^2\beta^{-3}\rangle$ for *i*=*a*,*b*,*c* with $\beta^2=\omega_n^2+\Delta^2$, Matsubara frequency ω_n, $\hat{v}_i=v_i/v_F$ and pair potential Δ in the uniform state. $v_F^2=\langle|\mathbf{v}|^2\rangle$, and $\langle A\rangle$ indicates the Fermi surface average of the quantity *A*. For γ=60, $m_a^{-1}=m_b^{-1}=0.498$ and $m_c^{-1}=1.38\times10^{-4}$ at low temperature T=0.1T_c. T_c is the transition temperature. We use Ginzburg-Landau parameter $\kappa=2.7$ appropriate to Sr_2RuO_4.

Magnetic field orientation θ dependence of the FLL form factors at $\bar{B}=0.8$, 1.5 and 3.0 are presented in Fig. 1. The FLL form factors in the London theory have weak $\bar{B}$-dependence. The overall behaviors are similar to those reported in previous work for YBCO with $\gamma\sim6$, $\kappa=100$, $\bar{B}=0.1$ and T=0.5T_c. The transverse component $|B_{tr(h,k)}|^2=|B_{x(h,k)}|^2+|B_{y(h,k)}|^2$ gives the intensity of spin-flip SANS at the spot (*h*,*k*). $|B_{tr(1,1)}|^2$ in Fig. 1(a) is more than 10 times larger than $|B_{tr(1,0)}|^2$ in Fig. 1(b). The maximum position of $|B_{tr(1,1)}|^2$ is shifted to larger $\theta(\sim80°)$, compared to the case of $\gamma\sim6$. The *z*-component $|B_{z(h,k)}|^2$ gives the intensity of conventional non-spin-flip SANS. As shown in Fig. 1(c), $|B_{z(1,1)}|^2$ has large intensity for $\bar{\mathbf{B}}\parallel c$ at $\theta=0$, and becomes very small for $\bar{\mathbf{B}}\parallel ab$ at $\theta=90°$, reflecting large anisotropy γ=60. Another $|B_{z(1,0)}|^2$ also shows similar behavior to $|B_{z(1,1)}|^2$.

3. Flux line lattice form factors in the Eilenberger theory, and the fitting by the extended London theory

In the Eilenberger theory, spatial structure of the pair potential $\Delta(\mathbf{r})$ and the internal magnetic field distribution $\mathbf{B}(\mathbf{r})=\nabla\times\mathbf{A}(\mathbf{r})$ are calculated from the Eilenberger equation [3,4]

$$\{\omega_n+i\mu B(\mathbf{r})+\hat{v}\cdot[\nabla+i\mathbf{A}(\mathbf{r})]\}f=\Delta(\mathbf{r})g,\quad\{\omega_n+i\mu B(\mathbf{r})-\hat{v}\cdot[\nabla-i\mathbf{A}(\mathbf{r})]\}f^+=\Delta^*(\mathbf{r})g, \tag{2}$$

with $g=(1-ff^+)^{1/2}$, coupled with the gap equation $\Delta(\mathbf{r})=g_0N_0T\sum_{0<\omega_n<\omega_c}\langle f+f^+\rangle$ and the current equation

$$\nabla\times\nabla\times\mathbf{A}(\mathbf{r})=-\kappa^{-2}2T\sum_{\omega_n>0}\langle\hat{\mathbf{v}}\,\mathrm{Im}\{g\}\rangle+\nabla\times(0,0,M_{para}),\quad M_{para}=M_0[B(\mathbf{r})-\mu^{-1}2T\sum_{\omega_n>0}\langle\mathrm{Im}\{g\}\rangle]/\bar{B}, \tag{3}$$

where, $g(\omega_n,\mathbf{p},\mathbf{r})$, $f(\omega_n,\mathbf{p},\mathbf{r})$, and $f^+(\omega_n,\mathbf{p},\mathbf{r})$ are quasi-classical Green's functions with Matsubara frequency ω_n.

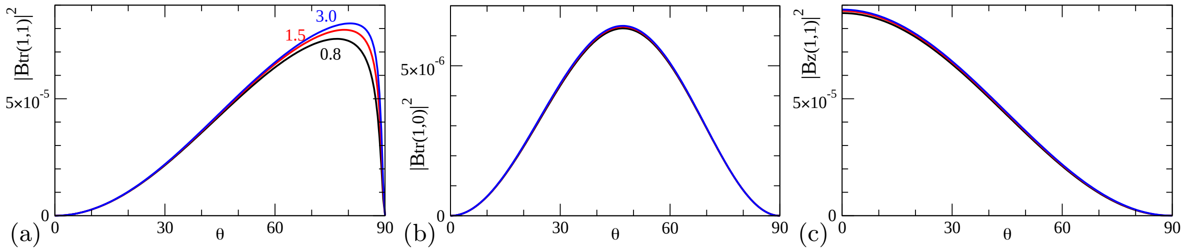

Fig. 1. (a) FLL form factors (a) $|B_{tr(1,1)}|^2$, (b) $|B_{tr(1,0)}|^2$, (c) $|B_{z(1,1)}|^2$ as a function of magnetic field orientation θ in the London theory. $\bar{B}$=0.8, 1.5, and 3.0 in the Eilenberger unit. Data points for three $\bar{B}$ are almost on the same line in (b) and (c).

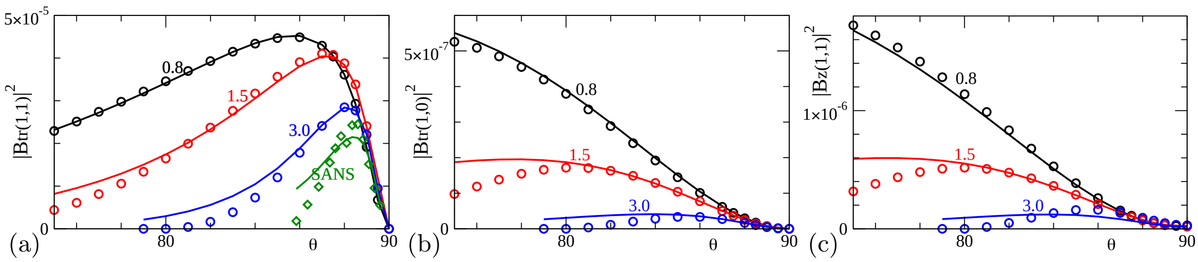

Fig. 2. (a) FLL form factors (a) $|B_{tr(1,1)}|^2$, (b) $|B_{tr(1,0)}|^2$, (c) $|B_{z(1,1)}|^2$ as a function of θ for $\theta > 75°$. $\bar{B}$=0.8, 1.5, and 3.0. We also show SANS data [1] in (a). Points are for the Eilenberger theory or SANS data. Lines are for the extended London theory.

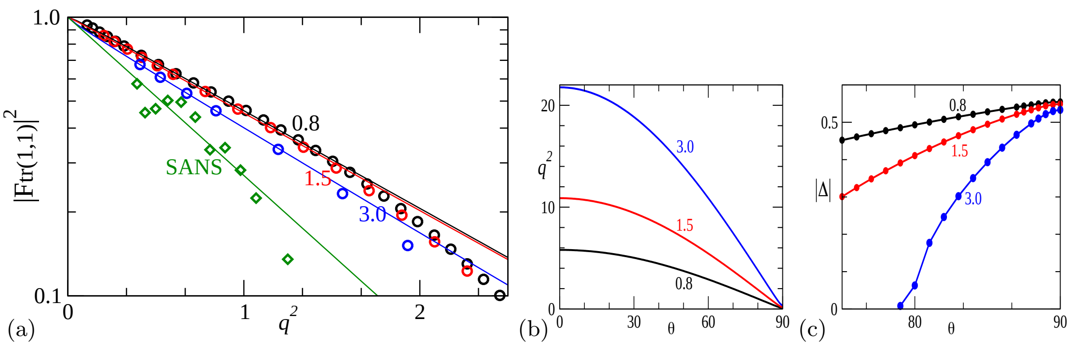

Fig. 3. (a) Points indicate cutoff function $|F_{tr(1,1)}|^2 = |B^{(E)}_{tr(1,1)}|^2/|B^{(L)}_{tr(1,1)}|^2$ as a function of q^2_{eff} for $\bar{B}$=0.8, 1.5, 3.0 and SANS data [1]. Lines are for the fitting by Eq. (5). (b) θ-dependence of q^2_{eff}. (c) θ-dependence of spatially averaged amplitude of the pair potential.

$M_0 = (\mu/\kappa)^2\,\bar{B}$. The pairing interaction and cut-off energy ω_c have a relation $(g_0 N_0)^{-1} = \ln T + 2T\sum_{0<\omega_n<\omega_c}\omega_n^{-1}$. We use the paramagnetic parameter $\mu = 0.04$. Using the same Fermi surface and parameters to those in Sec. 2, we calculate the FLL form factors from $\mathbf{B}(\mathbf{r})$ obtained by the Eilenberger theory. Since the vortex core structure is exactly calculated in this method, we can obtain quantitatively reliable results for the FLL form factors.

The FLL form factors in the Eilenberger theory are presented by points in Fig. 2. There, we present the case of low field $\bar{B}$=0.8 in addition to the cases of higher fields $\bar{B}$=1.5 and 3.0 [4]. The contribution of the paramagnetic pair breaking is negligible at $\bar{B}$=0.8 and 1.5, but the paramagnetic suppression of the pair potential appears at $\bar{B}$=3.0. In Fig. 2, we see eminent $\bar{B}$-dependence contrary to weak $\bar{B}$-dependence in the London theory. With increasing $\bar{B}$, the FLL form factors are suppressed. The maximum angle of the dominant transverse component $|B_{tr(1,1)}|^2$ in Fig. 2(a) is located at higher θ, compared to results of the London theory in Fig. 1(a). The minor transverse component

$|B_{tr(1,0)}|^2$ in Fig. 2(b) and longitudinal component $|B_{z(1,1)}|^2$ in Fig. 2(c) are decreasing functions in large θ range presented in Fig. 2 for $\bar{B}=0.8$. However, they has maximum at 80° and 85° for $\bar{B}$=1.5 and 3.0, respectively, since suppression occurs at lower θ. In Fig. 2(a), we also show experimental data on Sr_2RuO_4 at $\bar{B}/H_{c2}\sim 0.33$ ($\bar{B}$=0.5 [T], H_{c2}=1.5[T]). They are suppressed at lower θ, compared to the corresponding theoretical results for $\bar{B}$=3.0 ($\bar{B}/H_{c2}\sim 0.33$).

To discuss the discrepancy between the London theory in Fig. 1 and the Eilenberger theory in Fig. 2, we introduce the extended London theory [3]. There, quantitatively reliable form factors $|B^{(E)}_{tr(h,k)}|^2$ and $|B^{(E)}_{z(h,k)}|^2$ (points in Fig. 2) obtained in the Eilenberger theory are considered as

$$|B^{(E)}_{tr(h,k)}|^2 = |F_{tr(h,k)}B^{(L)}_{tr(h,k)}|^2, \quad |B^{(E)}_{z(h,k)}|^2 = |F_{z(h,k)}B^{(L)}_{z(h,k)}|^2, \tag{4}$$

where $|B^{(L)}_{tr(h,k)}|^2$ and $|B^{(L)}_{z(h,k)}|^2$ are form factors in Fig. 1 by the London theory. $|F_{tr(h,k)}|^2$ and $|F_{z(h,k)}|^2$ are cut-off functions reflecting contributions by the vortex core at the center of a flux line. In Fig. 3(a), we present $|F_{tr(1,1)}|^2 = |B^{(E)}_{tr(1,1)}|^2/|B^{(L)}_{tr(1,1)}|^2$ as function of $q^2_{eff}\equiv q_x^2+(q_y/\Gamma_\theta)^2$. The θ-dependence of q^2_{eff} is presented in Fig. 3(b). As for experimental data in Fig. 3(a), we use SANS data as $|B^{(E)}_{tr(1,1)}|^2$, and $|B^{(L)}_{tr(1,1)}|^2$ is at $\bar{B}$=3.0. Results (points) of the Eilenberger theory and the SANS data in Fig. 3(a) is fitted by lines of a function

$$|F_{tr(h,k)}|^2 = \exp(-c_1 q_{eff} - c_2 q^2_{eff}). \tag{5}$$

The fitting parameters determined in the range $q^2_{eff}<1$ are, respectively, (c_1, c_2) =(-0.0569, 0.830), (-0.0224, 0.785), (0.0776, 0.836) for $\bar{B}$=0.8, 1.5, 3.0. These are almost Gaussian functions, since c_1 is very small. These results for low T=0.1T_c and large γ=60 are contrasted with those for higher T=0.5T_c and smaller $\gamma\sim$6, where the term with c_1 is not negligible [1]. For the SANS data, we use a Gaussian function with c_2=1.308 assuming c_1=0.

In Fig. 2, we also show lines of the form factors estimated by the extended London theory in Eqs. (4) and (5) with fitting parameters shown in Fig. 3(a), assuming $|F_{z(1,1)}|^2=|F_{tr(1,0)}|^2=|F_{tr(1,1)}|^2$. At $\bar{B}$=0.8, lines and points are in nice accordance in the θ-dependence. However, at higher $\bar{B}$ and the SANS data, we see that points of the form factors are smaller than the lines at smaller θ range. These correspond to behaviors in Fig. 3(a), where data points deviate toward lower from lines of the fitting functions at $q^2_{eff}>1$. The deviations come from the θ-dependence of the pair potential in the Eilenberger theory, as shown in Fig. 3(c). The pair potential is suppressed at smaller θ, because the upper critical field H_{c2} is rapidly suppressed in the case of large γ. On the other hand, the pair potential is treated as a constant in the London theory. We note that the deviation between the Eilenberger theory and the SANS data comes from additional factors of the material, such as multi-band superconductivity [5].

From these results, we found that extremely large anisotropy ratio γ=60 leads to large differences between behaviors obtained by the London theory in Fig. 1 and by the Eilenberger theory in Fig. 2. These are because (i) the cutoff function in Eq. (5) gives large θ-dependence since variable range of q^2_{eff} in Fig. 3(b) is larger, and (ii) θ-dependence of the pair potential in Fig. 3(c) gives significant contributions.

4. Summary

We have studied the magnetic field orientation θ dependence of transverse and longitudinal FLL form factors at some field magnitude $\bar{B}$. While the $\bar{B}$-dependence is weak in the London theory, the quantitative estimate of the form factors becomes smaller at higher $\bar{B}$ in the Eilenberger theory. This $\bar{B}$-dependence can be included in the cutoff function of the extended London theory. However, there are still deviations from the extended London theory, because pair potential has θ-dependene by the suppression at smaller θ. These results give helpful information for analysis of the FLL form factors observed by the SANS experiments in uniaxial superconductors including Sr_2RuO_4.

References

[1] C. Rastovski, *et al.*, Phys. Rev. Lett. **111** (2013) 087003, 1-5.
[2] S. L. Thiemann, Z. Radovic, and V. G. Kogan, Phys. Rev. B **39** (1989) 11406-11412.
[3] Y. Amano, M. Ishihara, M. Ichioka, N. Nakai, K. Machida, Phys. Rev. B **90** (2014) 144514, 1-8.
[4] Y. Amano, M. Ishihara, M. Ichioka, N. Nakai, K. Machida, Phys. Rev. B **91** (2015) 144513, 1-13.
[5] N. Nakai and K. Machida, Phys. Rev. B **92** (2015) 054505, 1-12.